ELSEVIER

Catalysis Today 29 (1996) 437–442

CATALYSIS TODAY

Photocatalytic destruction of toluene and xylene at gas phase on a titania based monolithic catalyst

J. Blanco [a,*], P. Avila [a], A. Bahamonde [a], E. Alvarez [a], B. Sánchez [b], M. Romero [b]

[a] *Insto. Catálisis y Petroleoquimica. C.S.I.C., Campus UAM Cantoblanco, 28049 Madrid, Spain*
[b] *Insto. Energías Renovables. C.I.E.M.A.T, Madrid, Spain*

Abstract

Toluene and xylene were subjected to gas-solid heterogeneous photocatalytic oxidation on a titania based monolithic catalyst, in order to investigate the potential of solar-driven detoxification as a clean and safe method for air purification and gas phase waste destruction. Thus, gaseous streams with toluene or xylene were conducted through a monolithic catalysts based on titania dispersed on a fibrous silicate and irradiated with a Xenon lamp in the presence of air, at process temperatures from 150 to 450°C. Destructions levels higher than 96% were achieved for toluene and 99% for xylene at Area Velocity values in the range of 5–8 m h^{-1}. A non-negligible number of undesirable sub-products (furans and benzofurans) were identified in partial oxidation conditions. The concentration of these sub-products was higher in the thermal process than with the photocatalytic system. Textural properties of the catalyst, the nature of phases and their distribution on the surface and light absorption properties were studied using techniques such as mercury intrusion porosimetry, scanning electron microscopy (SEM-EDX), X-ray diffraction and diffuse reflectance UV–Vis. spectroscopy.

Keywords: Ti catalysts; Heterogenous photocatalytic oxidation; Solar driven detoxification

1. Introduction

The destruction of contaminants by photocatalytic means is one of the purification techniques having appeared in recent years which has achieved a singular importance due to its high effectiveness for the destruction of determined organic compounds at relatively low temperatures [1]. Although most of these studies have been carried out in aqueous media for the destruction of chlorinated compounds [2,3], recently an important study over the possibility of the destruction of Volatile Organic Compounds (VOC's) in the gas phase has appeared [4].

The utilization of monolithic catalysts — solid structures pierced by parallel channels — for these types of processes supposes an innovation of great importance, which permits on the one hand the reduction by several orders of magnitude of the pressure drop produced by the passage of the gas through the catalyst and on the other to significantly augment the irradiated surface and thus the photocatalytically active surface [5]. These facts permit the treatment of relatively large volumes of gas, with very low values of pressure drop whilst maintaining elevated levels of effectivity.

* Corresponding author. E-mail pavila@icp.csic.es

SSDI 0920-5861(95)00317-7

2. Experimental

2.1. Activity test

A stream of standard dry air (2.2 l/min) was mixed with toluene or xylenes (3000–6000 ppm). The reactor was made of stainless steel and had an effective aperture diameter of 8 cm enclosed with a quartz window. Inside the reactor was placed the monolithic catalyst (4 cm diameter × 2 cm length) in such a way that the light illuminates all the internal surface of the channels. Contaminants passed through the monolithic catalyst at a controlled temperature and outlet gases were analyzed by direct sampling (on-line) using a GC with a FID detector (Hewlett Packard 5890 Series II). At controlled time intervals, manually switched samples of outlet gases were adsorbed by using Tenax, for further GC–MS identification (Using a thermal desorption system Perkin Elmer, Model ATD 400 with a MS Hewlett Packard, 5971A MSD with HP 5890A GC). A 4000 W Xe lamp supplied incident flux (average 8 W/cm^2). A filter to remove $\lambda \leq 300$ nm was used. Inlet and outlet temperatures at the reactor were monitored with thermocouples located in non-illuminated positions.

2.2. Catalyst preparation and characterisation

A catalyst consisting of vanadium oxide impregnated on titanium dioxide (anatase) dispersed in magnesium silicate was prepared by extrusion from a paste composed of all the components as described elsewhere [6]. Previous studies demonstrated a better photocatalytic performance of the titania based catalyst when it is impregnated with VO_x [5]. The prepared square-cell monoliths have a pitch of 2.5 × 2.5 mm, 0.9 mm wall thickness and geometric surface of 8.2 cm^2 cm^{-3}.

The surface area of the catalyst was measured by nitrogen adsorption–desorption using the BET method in a Micromeritics ASAP 2100 D and the pore size distribution by mercury intrusion using a Micromeritics 9300 porosimeter. The morphology of the surface, as well as the average particle size was determined in a scanning electron microscope (SEM) JEOL JSM 6400. The nature of the phases on the catalyst were determined by means of a Philips PW 1730/10 X-ray diffractometer and diffuse reflectance UV–Vis. spectra were obtained in a Shimadzu model 2100 UV–Vis. spectrometer.

3. Results and discussion

The morphology of the catalyst surface can be seen in the micrograph presented in Fig. 1. The right half of this picture is the part of the photograph that appears within the rectangle in the left half, shown at a magnification factor of 5.

From the microscopy results it has been observed that this catalyst is made up of two types of particles. The first type, due to the natural silicate material, were fibrous particles with sizes ranging from 100 to 250 μm. These particles are in turn composed of bundles of fibres, which range in size from 0.2 to 1 μm in length and 0.01–0.1 μm in width.

The second type of particles, due to the TiO_2, were pseudo-spherical with sizes ranging from 0.05 to 0.1 μm, which can be found grouped together to form units of varying sizes

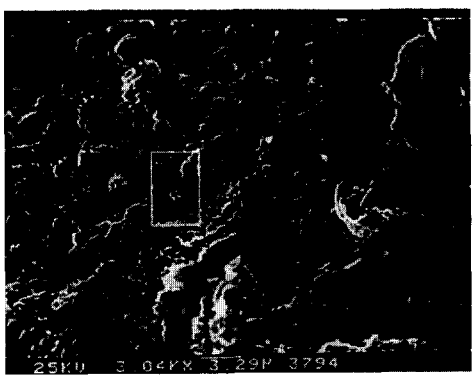

Fig. 1. Scanning electron micrograph of the internal surface of the catalyst.

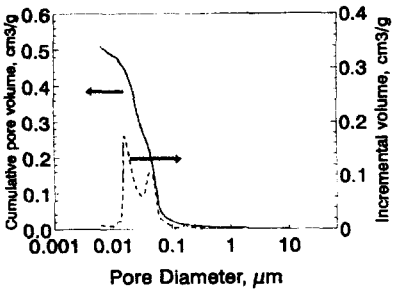

Fig. 2. Mercury porosimetry of the catalyst.

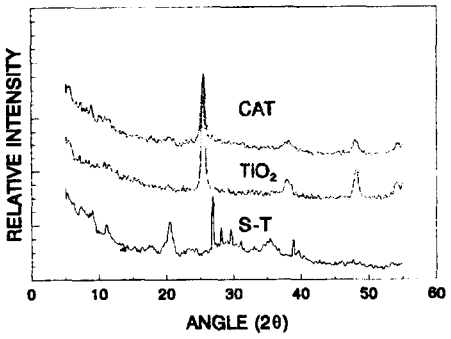

Fig. 3. X-Ray diffractograms of the catalyst 'Fot-1' and reference samples.

(0.3 to 1 μm), in which the original particles maintained their identity.

The particles of TiO_2, which are impregnated with the vanadium salt, are dispersed among the silicate fibres. The association of the vanadia to titania has been proven by EDX [7].

3.1. Textural properties

The catalyst obtained has the following textural properties:

Bulk density = 0.64 g cm^{-3}, total pore volume (MIP) = 0.5 cm^3 g^{-1} and BET surface area = 98 m^2 g^{-1}. In Fig. 2 the cumulative pore volume and pore size distribution curves of this catalyst are shown.

From these results it can be concluded that this catalyst has and important contribution of the mesoporosity, with a bimodal pore size distribution. The first corresponding to pores with diameters in the range 0.01–0.04 μm and the second to pores in the range 0.04–0.1 μm, being the maximum pore diameter of 0.02 and 0.08 μm, respectively.

This pore distribution can be explained in terms of spaces between fibres, bunches of fibres and particles of titania, 'pores' that have been created during the kneading and the thermal treatment [7].

3.2. Nature of phases

In Figs. 3 and 4, the X-ray diffraction and diffuse reflectance UV–Vis. spectra obtained for the catalyst, along with those corresponding to the products considered as references in this study, siliceous support 'S-T' and TiO_2 , all in the form of monoliths treated at 500°C are presented.

The XRD spectra obtained with this catalyst can be considered as a mixture of the natural silicate and titania precursors, no new phase was detected in its composition. Titania remains as anatase phase, and no formation of V_2O_5 was appreciated.

The results obtained by diffuse reflectance UV–Vis. spectroscopy indicated that in the zone of interest (300–600 nm) the TiO_2 has a strong absorption band between 300 and 370 nm. For its part the siliceous support (S-T) presented a less intense band than the TiO_2 in the same region (300–370 nm) but was much broader, with a residual absorption up to almost 800 nm.

The catalyst presented an intermediate behaviour, that is to say showing the advantages of both materials. In effect, in the zone located between 300 and 350 nm, the adsorption curve

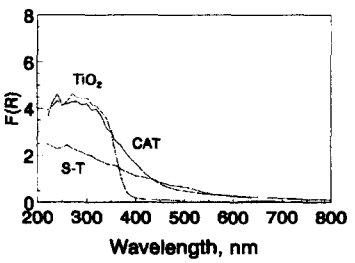

Fig. 4. Diffuse reflectance UV–vis. spectra of catalyst 'Fot-1' and reference samples.

was practically equal to that of the TiO_2. However, as with the siliceous support, the adsorption band was much broader and extended up to 600–800 nm. If the zone located between 350 and 600 nm is considered, the catalyst displayed a greater absorption capacity of this radiation than that of the purely TiO_2 sample, which could justify that it should have a greater activity in photocatalytic reactions in which radiation in these wavelengths were involved. Photocatalytic activity is always a combination of metal oxide activity and substrate form and composition. In this case, the substrate is a natural product with significant amounts of α-Fe_2O_3 (2%) which is photoactive [8] and together with the impregnated V_2O_5 and TiO_2 may have a synergetic effect.

3.3. Activity tests

In order to quantify and compare the possible destruction of toluene between 'thermal-catalytic' and 'photo-catalytic' processes, some tests with a Xenon lamp and without light, using the catalyst and in the absence of it, were carried out. Thermal- and photo-catalytic experiments were performed between 130 and 435°C because of several reasons: Temperatures above 500°C were conservatively avoided to protect V_2O_5 and TiO_2 (anatase). Temperatures below 130°C were not considered to avoid organic condensation, since we introduced contaminant concentrations in the thousands of ppm range (Fig. 5).

When the catalyst is absent, both with light and without it, the activity was absolutely negligible. When catalyst is present, the following results are obtained:

Below 200°C, there is a large difference between the efficiency of both processes. Whereas the photocatalytic tests show conversion values above 80% even at 130°C, the thermal catalytic process needs to operate at least at 200°C to obtain this grade of conversion.

At temperatures higher than 200°C, there are not significant differences between the toluene

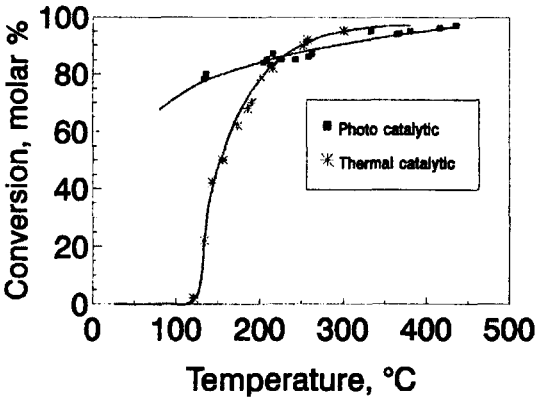

Fig. 5. Toluene destruction at thermal and photocatalytic conditions.

conversion values obtained by thermal and photocatalytic processes. Both exhibit destruction levels from 85% to 95%. However under these conditions, important differences are detected in the by-products generated by the two processes.

Table 1 summarizes the yields obtained for detected by-products in toluene oxidation at 260°C, when toluene destruction efficiencies are similar for both processes (90%). At these conditions, benzene, benzaldehyde and benzoic acid, together with some yields of 2,5-furandione and 1,3-isobenzofurandione were the only intermediates detected. There is a clear parallelism between these results and the results obtained by the atmospheric chemists using smog chambers where OH radicals are referred as the promoters of degradation steps.

The high yields of benzaldehyde formed in the photocatalytic reaction could be explained according to the schemes suggested by several

Table 1
Products identified in toluene catalytic oxidation (mol-%)

By-product	Thermocatalytic (260°C)	Photocatalytic (260°C)
Benzene	–	0.042
Benzaldehyde	0.286	0.643
2,5-Furandione	0.411	–
Benzoic acid	0.180	–
1,3-Isobenzofurandione	0.180	–

atmospheric chemists [9–17]. The by-products referred to in the literature by those authors are coincident with the by-products basically identified by GC–MS in our experiments and the OH radical role suggested is coincident with the mechanism usually proposed in photocatalysis with semi-conductors. This pathway includes the following steps: first, benzyl radicals are produced via H atom abstraction from the methyl group by OH radicals; the final transformation of benzyl radical into benzaldehyde strongly suggests the presence of benzyloxyl radicals. The step from benzyloxyl radical to benzaldehyde should be driven by oxygen and an additional redox reaction.

Atkinson et al. [10] suggested a new H atom abstraction from the substituent CHO group to form the benzoyl radical.

The production of substituted furans is postulated by Shepson et al. [15] and by Killus and Whitten [18] via intramolecular H atom transfer reaction of the initially formed radicals leading to ring cleavage.

Other ring fragmentation products reported in homogeneous phase tests with OH radicals [10], like glyoxal, methylglyoxal and by acetyl were not found in our catalytic tests. Phenolic compounds were also not detected.

Similar results were obtained for xylene destruction, but the destruction level under the same conditions, was of the order of 98–99%. The list of main by-products detected and their corresponding yields are shown in Table 2.

Methylbenzaldehyde was the most persistent compound (like benzaldehyde is in the case of toluene). This fact demonstrates the dominant pathway of OH radical reactions forming aldehydes from methyl groups. Substituted furans and benzofurans: 1,3-isobenzo-furandione and 2,5-furandione were also found in relatively high yields at low temperature (200°C) in the thermal tests. Photocatalytic tests revealed much lower yields of furans (< 0.5%). Methylbenzaldehyde and furans were also reported by Shepson et al. [15].

Finally, photocatalytic tests carried out at 400°C achieved 99% xylene degradation with very low concentration of by-products, which demonstrates the possibility of destruction of these compounds by this process with high efficiency.

4. Conclusions

Concentrations of VOCs in air in the thousands of ppm range may be destroyed using gas/solid heterogeneous photo-oxidation with $MgSiO_x/TiO_2/VO_x$ monolithic catalysts.

An range of temperatures below 200°C has been identified where photo-catalysis plays an

Table 2
Products identified in xylene catalytic oxidation (mol-%)

By-product	Thermocatalytic (200°C)	Photocatalytic (250°C)	Photocatalytic (400°C)
Toluene	–	< 0.1	0.18
Benzaldehyde	2.36	1.73	< 0.1
2,5-Furandione	0.94	0.45	–
Methyl-benzaldehydes	1.04	1.45	–
Benzoic acid	[a]	[a]	–
Methyl-benzoic acids	1.35	0.15	–
Benzene dicarboxaldehyde	–	0.20	–
1,3-Isobenzofurandione	2.4	0.44	–

[a] Difficult resolution, but significant yield.

important role and where further optimization studies should be focused.

A non-negligible number of undesirable by-products could be identified below 400°C. High yields of aromatic aldehydes were obtained. A second group of substituted furans and benzofurans was identified in partial oxidation conditions, with thermal catalysis producing more of these intermediates than photo-catalysis. Unlike smog chamber homogeneous phase tests reported in the literature, we did not find significant amounts of either phenolic compounds (e.g., *o*-cresol) or ring cleavage products such as methylglyoxal, glyoxal and byacetyl. Since benzaldehyde is a persistent compound at high temperatures, further work needs to be done in this area.

From these results it can be concluded that the use of these types of monolithic catalysts rise significant advantages not only concerning pressure drop and improvement of chemical and photonic contact surface but also from the point of view of the by-products formed and efficiencies.

Acknowledgements

This work has been partially supported by the EC Environment Program, project No. EV5V-CT94-0558.

References

[1] D.F. Ollis and Al-Ekabi H. (Editors), Photocatalytic Purification and Treatment of Water and Air, Elsevier, Amsterdam, 1993.
[2] D.F. Ollis, Photochemical Conversion and Storage of Solar Energy, Kluwer, Dordrecht, 1991, pp. 593–622.
[3] D.F. Olis, E. Pelizzetti and N. Serpone, in N. Serpone and E. Pelizzetti (Editors), Photocatalysis; Fundamentals and applications, Wiley, New York, 1989, pp. 603–638.
[4] J. Peral and D.F. Ollis, J. Catal., 136 (1992) 554.
[5] B. Sanchez, M. Romero, A. Vidal, M. Sanchez, A.L. Verdejo and P. Avila, Proc. 6th Int. Symp. Solar Thermal Conc. Tech., 2 (1992) 1211.
[6] J. Blanco, P. Avila, A. Bahamonde, C. Barthelemy, C. Chacón and J.M. Ramos, Sp. Patent No. 8803453, 1988.
[7] P. Avila, J. Blanco, A. Bahamonde, J. Palacios and C. Barthelemy, J. Mater Sci., 28 (1993) 4113.
[8] E. Pelizzetti, C. Minero and V. Maurino, Adv. Colloid Interf. Sci., 32 (1990) 271.
[9] H.A. Akimoto, M. Hoshino, G. Inoue, M. Okuda and N. Washida, Bull. Chem. Soc. Jpn., 51 (1978) 2496.
[10] R. Atkinson, W.P.L. Carter, D.R. Darnall, A.M. Winer and J.N. Pitts, Int. J. Chem. Kinet., 12 (1980) 779.
[11] A.C. Besemer, Atmos. Environ., 16(6) (1982) 1599.
[12] D.G. Hendry, NBS Spec. Publ. (US), 557 (1979) 85.
[13] M. Hoshino, H. Akimoto and M. Okuda, Bull. Chem. Soc. Jpn., 51 (1978) 718.
[14] T. Ibusuki and K. Takeuchi, Atmos. Environ., 20(9) (1986) 1711.
[15] P.B. Shepson, E.O. Edney and E.W. Corse, J. Phys. Chem, 88 (1984) 4122.
[16] K. Suzuki, S. Satoh and T. Yoshida, Denki Kagaku, 59(6) (1991) 521.
[17] H. Tagaki, N. Washida, H. Akimoto, K. Nagasawa, K, Y. Usui and M. Okuda, J. Phys. Chem., 84 (1980) 478.
[18] J.P. Killus and G.Z. Whitten, Atmos. Environ., 16(8) (1982) 1973.